Influence of boundary structure on cellular nucleation in Cu-3 w/oTi age-hardening alloys

N. Boonyachut · D. E. Laughlin

Abstract The kinetics of cellular precipitation at the grain boundaries in a Cu-3 w/o Ti alloy was investigated using the Johnson–Mehl–Avrami (JMA) model. The experimental results are well described by Cahn's site saturation model, showing that the initiation of cellular colony precipitation is limited by the availability of the nucleation sites. Orientation imaging microscopy (OIM) and transmission electron microscopy (TEM) analyses show that not all high angle grain boundaries contain preferred nucleation sites. It was observed that grain boundaries in aged alloys that do not have cellular colonies tend to have a special coincident site lattice (CSL) relationship.

Introduction

It is widely accepted that high-angle grain boundaries are the most likely sites for the initiation of cellular colony precipitation. However, grain boundaries are complicated due to the relationship between grain boundary structure, mobility, and energy. Several studies have been performed on the influence of the boundary structure on grain boundary precipitation. Matsuoka et al. [1] have shown that only grain boundaries with minimum of 22° misorientation are likely to initiate cellular precipitation in Cr–Ni

N. Boonyachut (✉)
Department of Primary Industries and Mines,
Ministry of Industry, Bangkok, Thailand
e-mail: nan_boonyachut@alumni.cmu.edu

D. E. Laughlin
Department of Materials Science and Engineering,
Carnegie Mellon University, Pittsburgh, PA 15213, USA
e-mail: Laughlin@cmu.edu

austenitic stainless steel. The absence of cellular colony on coherent twins and other low-energy and low-mobility boundaries has also been reported [2, 3]. In contrast, Manna et al. [4] observed cellular precipitation on coherent twins in Cu–Mg system. Thus, there seems to be no general rule of the role of grain boundary structure on the nucleation and growth of the cellular reaction. In this article, we investigate the character of the grain boundaries which either act or do not act as sites for initiation of the cellular precipitation process in the Cu-3 w/o Ti alloy.

Experimental

Samples of Cu–Ti alloys containing 3 w/o Ti were cut into small cubes about 10 mm in dimension. Each sample was solutionized at 800 °C for 1–2 h in flowing argon, followed by a water quench. Isothermal aging with temperatures ranging from 450 °C to 525 °C was carried out in a salt bath with a temperature variation of about ±2 °C. Bulk samples for quantitative analysis and orientation imaging microscopy (OIM) were mechanically polished and etched with Methanol-50 vol% Nitric acid (HNO_3).

The electron backscatter diffraction (EBSD) scans were performed on a XL40 FEG-SEM with a field emission gun. The EBSD scans of each sample containing at least 30,000 grains were performed with a step size of 2 micron. A dilation method with a 5 degree tolerance and 2 pixel size (default) was used for a routine clean up of each scan. Samples of Cu-3 w/o Ti with two different aging treatments were chosen to perform orientation measurements with the OIM technique, namely:

(1) 450 °C/50 h and
(2) 510 °C/2 h.

Both samples had a similar amount of cellular precipitation (∼2%), so the effect of aging temperature and under cooling could be compared. These low cellular colony fraction samples were also selected in view of fact that in them it was easier to identify the grain boundary from which the cellular colony had grown. In order to study the preferences of cellular precipitation on grain boundaries, the misorientation of each of the grain boundaries with their corresponding cellular colonies was determined. The misorientation of a grain boundary between the two selected grains were determined by using TSL^{TM} software. A total of 856 grain boundaries with cellular colonies were investigated in the sample aged at 450 °C, and 1,289 grain boundaries were investigated in the sample aged at 510 °C.

Samples of the early stages of precipitation and also after site saturation occurrence were prepared and investigated by transmission electron microscopy (TEM) in order to clarify the OIM results. Thin foils for TEM were prepared by mechanical grinding, followed by double-jet electropolishing. Methanol-33 vol% Nitric acid (HNO$_3$) was used as the electrolyte and the electropolishing was done in the range from −50 °C to −30 °C. A JEOL 2000 EX operated at 200 kV equipped with a double tilt holder with tilting capabilities of ± 40° was used for the orientation measurements. In this study, the orientations of the grains on each side of the grain boundary were determined from their selected area diffraction patterns (SADP). The selected area diffraction aperture (20 μm.) was inserted to insure that the electron beam diffracted only from the grain of interest. The sample was tilted until the SADP of both grains of the grain boundary of interest were on or close to a zone axis.
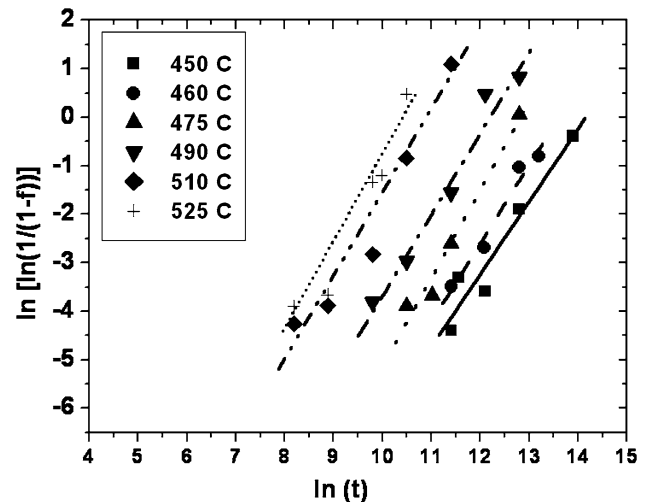
Results

Kinetics results

From the volume fraction of cellular precipitation versus time plots, the overall kinetics of the cellular precipitation can be expressed by the kinetic model of Johnson–Mehl–Avrami (JMA) [5]. The form of the JMA equation used was:

$$f = 1 - \exp[-(kt)^n] \tag{1}$$

From the Eq. 1, it can be seen that a plot of ln ln [1/(1 − f)] versus ln (t) should yield a straight line with a slope of n and an intercept of k. This was observed in our samples as shown in Fig. 1. The values of k and n obtained from the plots are summarized in Table 1. The values of n range between 1.5 and 1.9 which are different than the values of n of typical randomly distributed heterogeneous nucleation controlled by interface control which is ∼3–4 [6, 7].

Fig. 1 Plots ln ln[1/(1 − f)] versus ln(t) for various aging temperatures

Table 1 Summary of the slope values n and reaction rate k values

Temp °C	n	k (1/s)
450	1.5	7.08 E-07
460	1.62	1.23 E-06
475	1.81	2.69 E-06
490	1.67	5.25 E-06
510	1.72	1.66 E-05
525	1.93	2.86 E-05

Cahn [8] has derived a nucleation and growth rate model for grain boundary nucleation reaction such as cellular precipitation. In his study, Cahn showed that for a very high super saturation (large undercooling), a process called site saturation must be taken into account. In other words, if the initial rate of nucleation is very high, the grain corners, grain edges or the grain boundaries may be completely covered with nuclei in the early stage of transformation. Thus, the transformation rate of grain corner nucleation would be

$$f = 1 - \exp\left[-\left(\frac{4}{3}\pi C v^3 t^3\right)\right]$$

and the transformation rate of grain edge nucleation would be:

$$f = 1 - \exp\left[-(\pi L v^2 t^2)\right]$$

and the transformation reaction rate with the grain boundary nucleation would be of the form:

$$f = 1 - \exp[-(2Svt)]$$

where S is the boundary area per unit volume, L is the edge length per unit volume, C is the grain corner number per unit volume and v is the steady state growth rate.

The value of n depends on two factors: whether nucleation is occurring and the dimensionality of the growth of the new phase or constituent. Our experimentally determined values of n ranged between 1 and 2. This could happen if the corners and edges were saturated early, and the cellular regions started off being nucleated at grain boundaries and mainly growing in one dimension (from the boundary) yielding a value of $n = 2$. When site saturation occurred at the boundary, the value of n would fall to 1. The overall value of n thus would fall between 1 and 2 as we observed. The numbers of nucleation site (in this case the number of cellular colonies) for each aging temperature were counted, and the time at which site saturation occurs (constant number of nucleation sites) was determined. Figure 2 shows the plot between the number of nucleation sites versus time fraction (time/time to complete cellular precipitation reaction). Table 2 shows the site saturation time for each sample.

However, even when site saturation occurs, there are some grain boundaries that do not have any cellular nuclei. Figure 3 is an optical micrograph of Cu-3 w/o Ti aging at 510 °C for 10 h, which has become site saturated, and yet
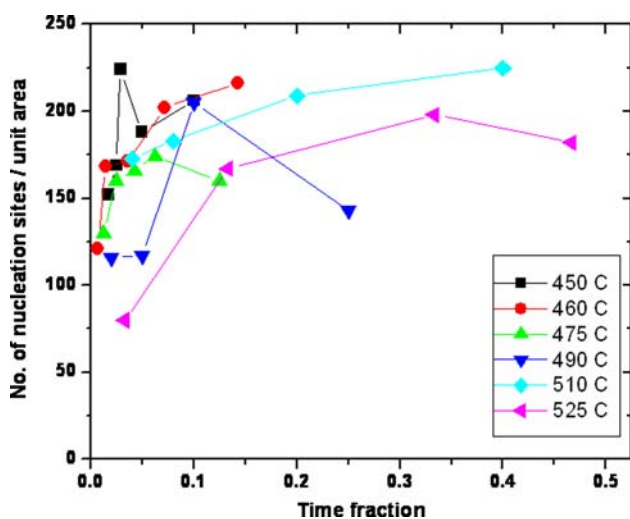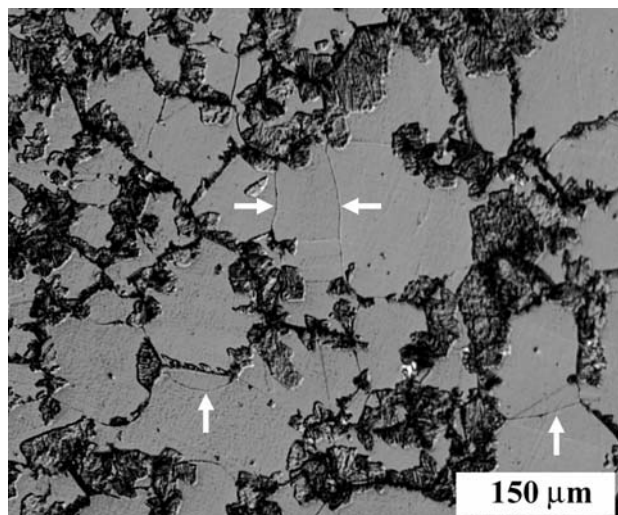

Fig. 3 An optical micrograph of a sample that has reached site saturation (no further nucleation). The arrows show grain boundaries with no cellular colonies

Fig. 2 Number of nucleation sites per unit area versus aging time (fraction) for different aging temperatures

Table 2 Volume fraction of cellular precipitation and aging time when site saturation is observed

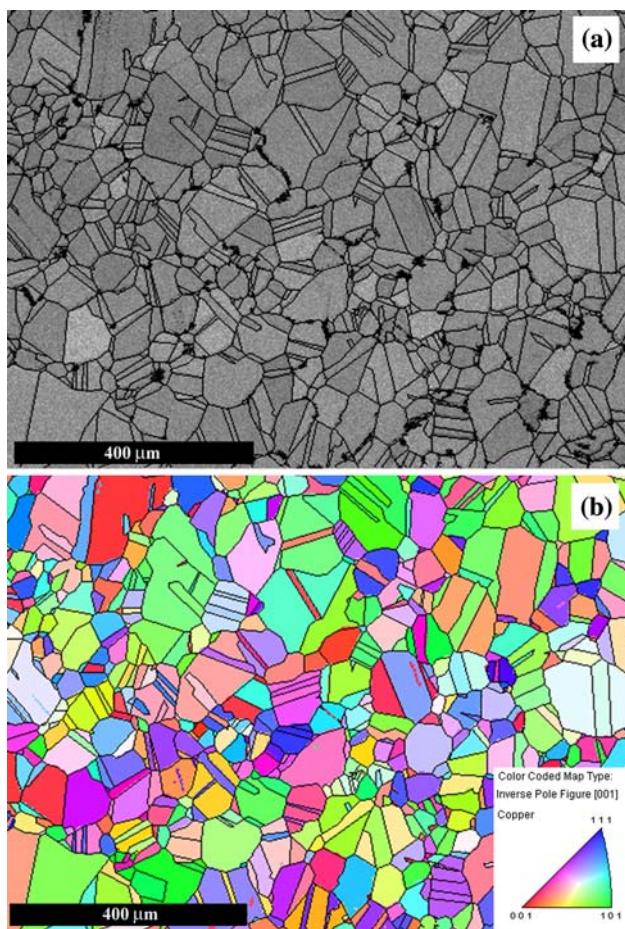| Temperature (°C)	Time (h)	Cellular precipitation (%)
450	100	14
460	100	30
475	50	25
490	25	14
510	10	35
525	5	23

there are grain boundaries that have no cellular colonies associated with them as indicated by the arrows. We investigated the character of these boundaries.
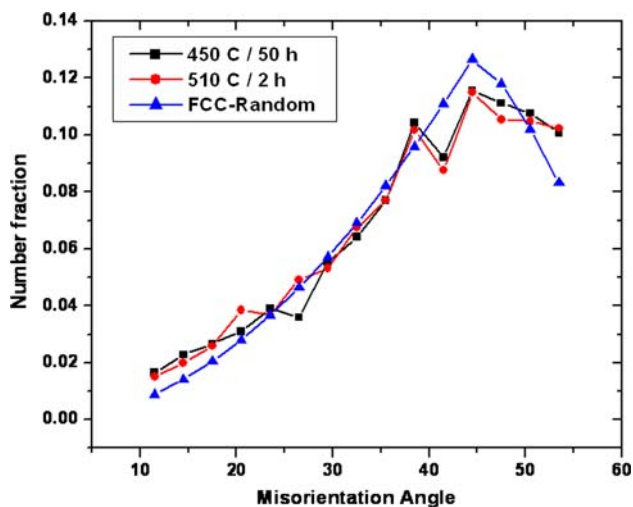
Orientation imaging microscopy (OIM)

The grain orientations in the samples were collected and mapped by the OIM system. Figure 4a shows the SEM image of a scanned area (450 °C/50 h) with an overlay of reconstructed grain boundaries. Figure 4b shows the color map of the inverse pole figure in the scanned area the same as a. From the orientations collected, the grain boundary misorientation distribution can be calculated and plotted in Fig. 5. The grain boundary misorientation distributions of both samples (450 °C/50 h and 510 °C/2 h) are basically the same. By comparing them with the Mackenzie distribution [9], it can be seen that the grain boundary misorientations are nearly randomly distributed. Figure 5 represents the grain boundary misorientation of both samples compared with randomly distributed cubic grains.

If cellular precipitation nucleates randomly, it is expected that the misorientation distribution of the grain boundaries that contain cellular colonies will follow the random distribution of Mackenzie (solid line). However, as seen in Fig. 6, in the early stages of the reaction (volume fraction of cellular precipitation ~2%), the cellular precipitation does not nucleate randomly on all grain boundaries of all misorientations, but nucleates on grain boundaries with preferential misorientations. Between the misorientations from 20° to 30°, the frequency of the presence of cellular precipitation is higher while from 30° to 45° it is lower. The aging temperatures between 450 °C
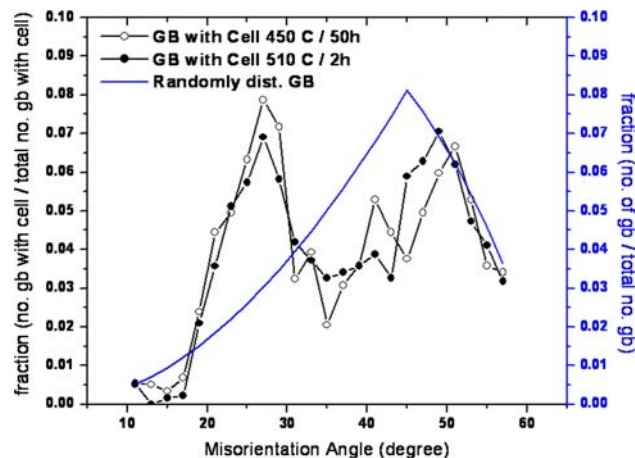
Fig. 4 a The SEM image of the scanned area and **b** the inverse pole figure map of the scanned area

Fig. 6 Misorientation distributions of all the grain boundaries that contain cellular colony compared with random set of misorientations (Mackenzie plot), showing that the grain boundaries that contain cellular colonies nuclei are not randomly distributed

and 510 °C do not have any significant differences in the cellular precipitation nucleation sites.

It is believed that only random high angle grain boundaries are suitable for nucleation due to their high grain boundary energy. From this study, there is no evidence of cellular colonies on twin boundaries which are considered "special boundary" with very low energy. However, as seen from the OIM results, not all random high angle grain boundaries are equally suitable for cellular nucleation. This suggests that there is some preference in nucleation for cellular precipitation and that might be due to the differences in the grain boundary structure and energy.

Observation of grain boundaries without presence of cellular precipitation

As shown earlier in Fig. 3, even after site saturation has occurred, there are some grain boundaries that do not have any cellular colonies associated with them. In this section, grain boundaries with no cellular colonies are investigated. The orientation of each grain was indexed, and the misorientation between both grains was determined. From the TEM results it is found that the grain boundaries that have no cellular colony are usually those that are special coincident site lattice (CSL) boundaries. All the misorientation relationships of grain boundaries investigated are summarized in Table 3.

Figure 7a shows a TEM bright field image of grain boundary #1 that has no cellular colony and b the SADP from both sides of the grain boundary. From the SADP, the orientation relationship between both grains is determined and is summarized in Table 3.

By comparing the angle/axis misorientation as shown in Table 3 with the list of axis/angle pair of CSL boundaries

Fig. 5 The grain boundary misorientation distribution of both samples compared with random set of orientations (Mackenzie plot), showing that in both samples the grain boundary misorientation is nearly randomly distributed

Table 3 Orientation relationships between grains of the investigated grain boundaries

Grain boundary number (#)	Orientation relationship		Misorientation		CSL	Deviation angle θ_m
	Direction $[uvw]_1//[uvw]_2$	Plane $(hkl)_1//(khl)_2$	Rotation axis $[d_1\ d_2\ d_3]$	Rotation angle (ω)		
1	$[1\ 1\ 0]_1//[3\ 2\ 1]_2$	$(-1\ 1\ 1)_1//(-1\ 1\ 1)_2$	$[-1\ 1\ 1]$	40.9°	$\sum7$ (38.2) [1 1 1]	2.69
2	$[2\ 1\ 1]_1//[4\ 1\ -1]_2$	$(3\ -5\ -1)_1//(2\ -4\ 4)_2$	$[15\ 2\ -1]$	32.6°	–	–
3	$[4\ 1\ 1]_1//[1\ 1\ 0]_2$	$(-1\ 5\ 9)_1//(-2\ 2\ -10)_2$	$[-5\ 12\ 22]$	34.2°	–	–
4	$[3\ 1\ 0]_1//[2\ 1\ 1]_2$	$(1\ -3\ 1)_1//(1\ -3\ 1)_2$	$[1\ -3\ 1]$	25.4°	$\sum45a$ (28.62) [3 1 1]	3.22 too high
5	$[2\ 1\ 1]_1//[2\ 1\ 1]_2$	$(5\ -13\ 3)_1//(1\ -1\ -1)_2$	$[2\ 1\ 1]$	52.7°	$\sum31b$ (52.29) [2 1 1]	0.41
6	$[0\ 0\ 1]_1//[0\ 0\ 1]_2$	$(2\ 8\ 0)_1//(-2\ 8\ 0)_2$	$[0\ 0\ 1]$	28.8°	$\sum17a$ (28.07) [1 0 0]	0.73
7	$[4\ 1\ -1]_1//[2\ 1\ 1]_2$	$(1\ -3\ 1)_1//(1\ -3\ 1)_2$	$[1\ -3\ 1]$	39.7°	$\sum23$ (40.45) [3 1 1]	0.75
8	$[2\ 1\ 1]_1//[2\ 1\ 1]_2$	$(0\ -2\ 2)_1//(-1\ 1\ 1)_2$	$[1\ 5\ 1]$	42.8°	$\sum49b$ (43.57) [5 1 1]	0.77
9	$[1\ 1\ 0]_1//[1\ 1\ 0]_2$	$(4\ -4\ 2)_1//(-4\ 4\ 2)_2$	$[1\ 1\ 0]$	32.4°	$\sum27b$ (31.59) [1 1 0]	0.81
C1	$[2\ 1\ 1]_1//[1\ 1\ 1]_2$	$(-4\ 2\ 6)_1//(-6\ 2\ 4)_2$	$[-5\ -12\ 5]$	22.5°	–	–
C2	$[4\ 1\ 1]_1//[2\ 1\ 1]_2$	$(-4\ 6\ 2)_1//(1\ 3\ -7)_2$	$[1\ 2\ -7]$	40.3°	–	–
C3	$[0\ 0\ 1]_1//[1\ 1\ 1]_2$	$(6\ -8\ 0)_1//(-8\ 6\ 2)_2$	$[19\ 22\ -4]$	55.3°	–	–

[10], it can be determined that the boundary is close to a CSL orientation of Σ7 (38.21° [1 1 1]) with deviation of 2.69°. A grain boundary can be defined as a near-CSL orientation if the deviation between the calculated misorientation value and the theoretical CSL misorientation is within the Brandon criterion [11] which is:

$$\theta_m < \frac{15°}{\sqrt{\Sigma}} \tag{2}$$

where θ_m is the deviation angle and $\sum$ is the number of reciprocal of normal lattice sites per coincidence lattice sites.

This grain boundary, with deviation of 2.69°, is within the Brandon criterion of Σ7 that is 5.67°. The deviation angle θ_m can be calculated from the misorientation matrix and the CSL orientation matrix as follows:
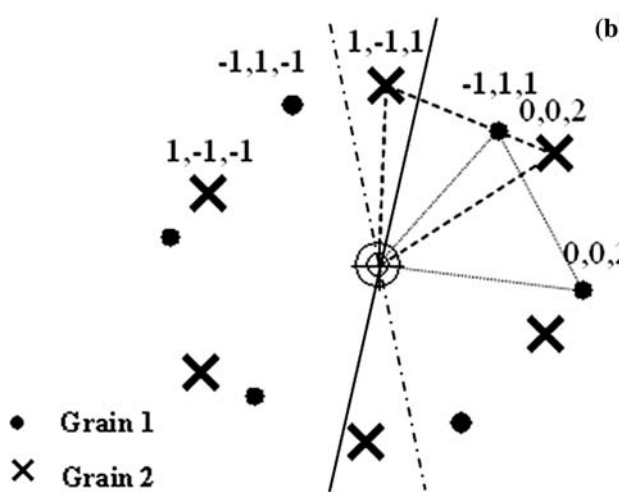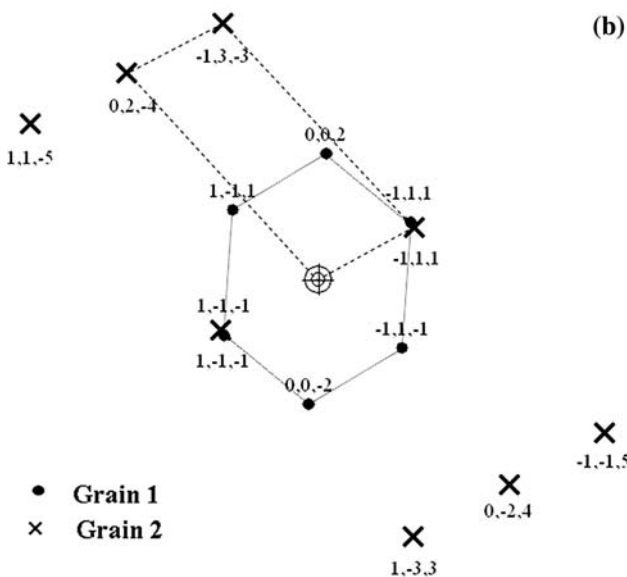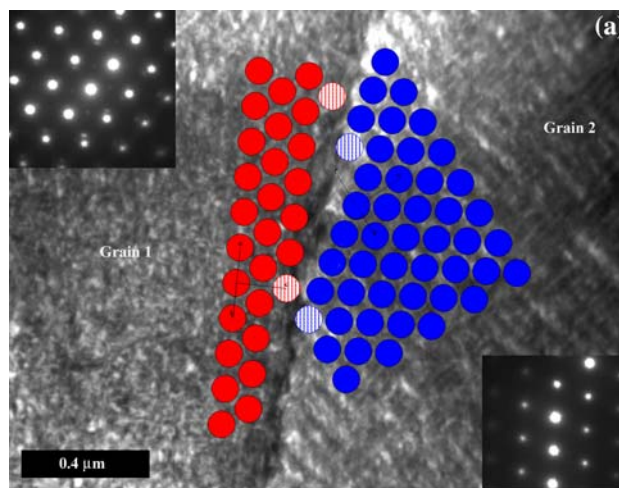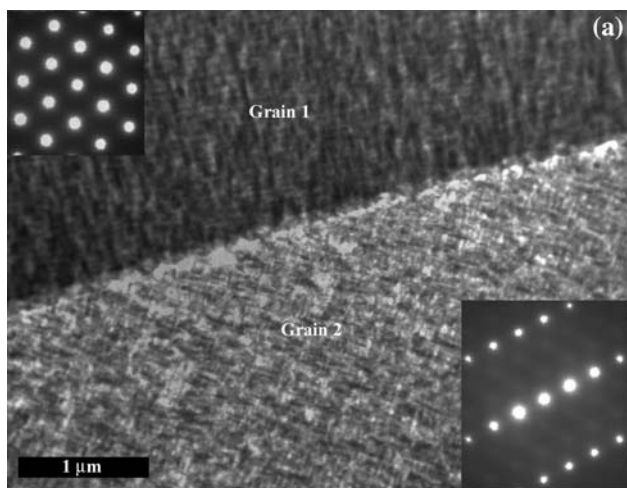
$$\cos(\theta_m) = \frac{\{\text{trace}(\Delta g \cdot \Delta g_{CSL}^T) - 1\}}{2} \tag{3}$$

where Δg is the misorientation matrix, and Δg_{CSL}^T is the CSL orientation matrix.

A site-saturated sample aged at 450 °C for 100 h was investigated. Figure 8a shows TEM bright field image of grain boundary #9 that has no cellular colony and b the SADP of both sides of the grain boundary. The orientation relationship between both grains and the misorientation of grain boundary #9 is shown in Table 3. The boundary is near a CSL orientation of Σ27a (31.59° [1 1 0]). Because both grains have the same plane normal perpendicular to the surface (same zone axis//beam), these two grains have a tilt relationship. If the grain boundary observed in the TEM was exactly perpendicular to the surface, this grain boundary would be identified as an "asymmetrical tilt"

boundary due to the fact that the grain boundary trace (solid line in Fig. 8b) was out of the mirror plane (dash-dot line in Fig. 8b) of the tilt axis. Assuming that the grain boundary trace is perpendicular to the surface, the grain boundary planes can be determined. Figure 9 shows a good atomic matching between two planes at the grain boundary, the red and the blue atoms correspond to grain 1 and grain 2, respectively. This good atomic matching in the boundary plane is a possible explanation as to why the CSL type grain boundaries have lower frequency of cellular precipitation.

Figure 10 summarizes the misorientation of the grain boundaries that do not have cellular colonies obtained by TEM technique including samples that were not site saturated (cross, grain boundaries #1–#7) and samples that were site saturated (star). Note that the grain boundary misorientation of grain boundaries from #1 to #7 spread from 25° to 53° of misorientation. However, four of the boundaries (#2, #3, #7, and #1) fall in the range of misorientation of 30° to 45° that have a smaller frequency of cellular precipitation as shown by the OIM. Grain boundaries #4, #5, and #6 fall close to the misorientation angles that have been observed to have a high frequency of cellular precipitation. However, it is important to keep in mind that this TEM sample was aged at 460 °C for 50 h, and it has not yet reached site saturation. In the samples that have been already site saturated, the grain boundaries that do not have any cellular colonies (#8 and #9) still fall in the range where there is a low frequency of cellular precipitation in the misorientation distribution (30°–45°). Both of them either have a special misorientation relationship or belong to a CSL boundary (in this case Σ27a and Σ49b with a tilt relationship).

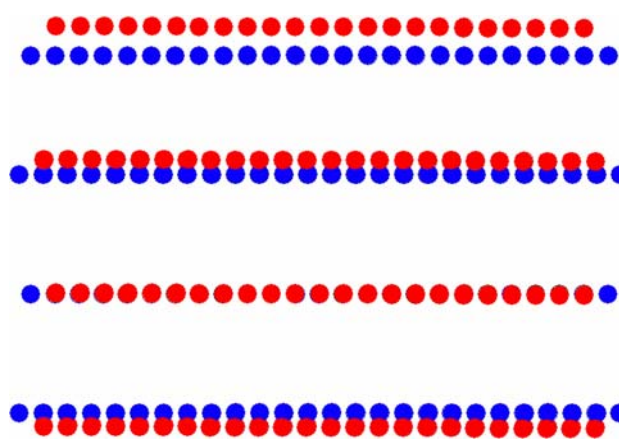Fig. 7 **a** Grain boundary #1 with no cellular colonies from a sample aged at 460 °C for 50 h (has not been site saturated) and **b** superimposed SADP of both grains

Fig. 8 **a** Grain boundary with no cellular colonies aged at 450 °C for 100 h and and **b** superimposed SADP of both grains

Observation of grain boundaries with the presence of cellular precipitation

Grain boundaries with cellular colonies have also been investigated. It is observed that grain boundaries with cellular colonies are mostly random high angle grain boundaries. Figure 11a shows grain boundary C2 that has a cellular colony and b the SADP of both sides of the grain boundary. From the SADP the orientation relationship between both grains was found to be as shown in Table 3.
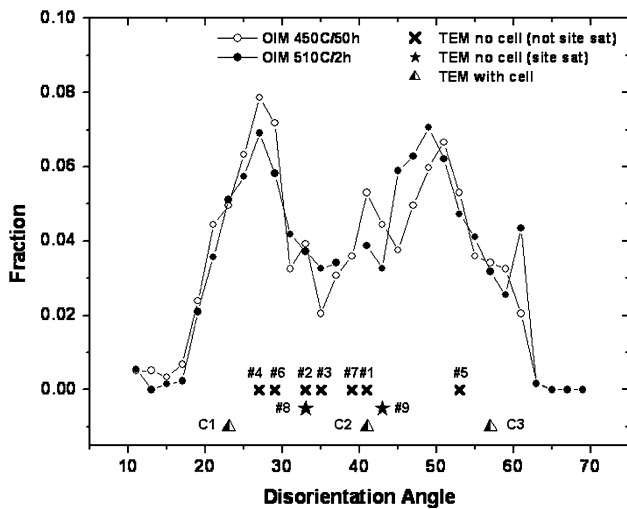
This misorientation is a normal high angle grain boundary and does not correspond to any special CSL boundary. Even though this grain boundary C2 has a misorientation in the range where there are relatively lower

Fig. 9 The good atomic matching between the two planes of the grain boundary

frequencies of cellular sites at the early stages than at the random stage, this grain boundary is just a normal high angle grain boundary.
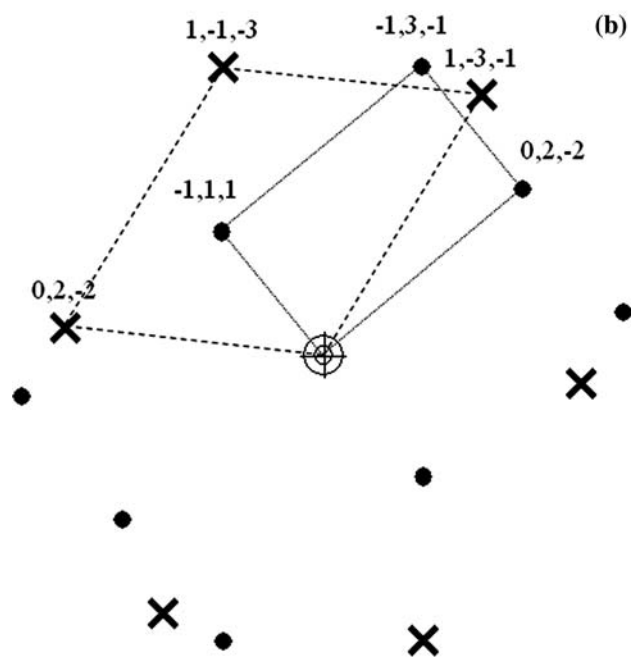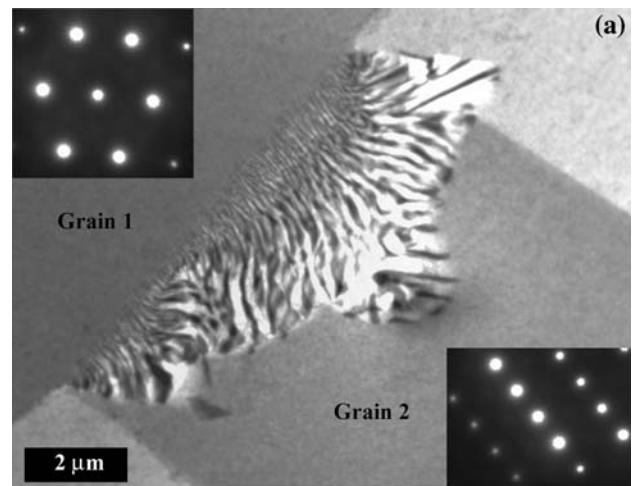
Fig. 10 Misorientation distributions of grain boundaries containing cellular colonies. Comparison between OIM/EBSD and TEM results

Figure 10 summarizes the misorientation of the grain boundaries that have cellular colonies, obtained by TEM technique (triangles) in comparison with the misorientation distribution of the grain boundaries that contain cellular colony obtained by OIM. As shown in these results, the misorientation of grain boundaries that contain cellular colonies C1, C2, and C3 fall in a wide range of misorientation angles, and the grain boundaries C1–C3 are normal high angle grain boundaries.

Summary and discussion

The kinetics of cellular precipitation using JMA relation is explained well by Cahn's site saturation model. The reaction of cellular precipitation is limited by preferred nucleation sites and conforms to a site saturation model.

The results obtained from both OIM (EBSD) and TEM techniques show that in the later stages of precipitation, when site saturation has occurred, the grain boundaries that have no cellular colonies have a special CSL relationship, which agrees with the studies on Al–Zn–Mg alloy done by Butler and Swann [12], and Unwin and Nicholson [13]. This is due to the fact that when two grains have a relationship close to CSL type, there is a high density of coincidence sites at the grain boundary. As a result of the "good fit", the grain boundary energy is expected to be low. Therefore, nucleation is not preferable at the boundaries with CSL relationships. This explains why nucleation sites at grain boundaries are not random, but selective. Also, it can be concluded that, not "all" high angle grain boundaries are suitable for nucleation of cellular colonies. Moreover, as the diffusion path during cellular precipitation is along the grain

Fig. 11 a Grain boundary C2 with cellular colonies and b superimposed SADP of both grains

boundary, such grain boundaries will have lower diffusion rates in some directions, further reducing growth processes that depend on diffusion.

However, the grain boundary plane (inclination) and other factors such as the orientation between precipitates habit plane and the grain boundaries are also believed to have a significant influence on the precipitation of cellular colony, and therefore require further study.

References

1. Matsuoka S, Mangan MA, Shiflet GJ (1994) In: Johnson WC (ed) Solid–solid phase transformations. The Minerals, Metals and Materials Society, Warrendale, PA, p 521
2. Vaughan D (1968) Acta Metall 16:563
3. Hornbogen E (1972) Met Trans 3:2717
4. Manna I, Pabi SK, Gust W (1991) J Mater Sci 26:4888. doi: 10.1007/BF00549866
5. Porter DA, Easterling KE (1992) Phase transformation in metals and alloys. Chapman and Hall, New York
6. Christian JW (1975) The theory of transformations in metals and alloys: part I, equilibrium and general kinetic theory. Pergamon Press, New York
7. Bunge HJ (1982) Texture analysis in materials science. Butterworths, London
8. Cahn JW (1956) Acta Metall 4:449
9. Mackenzie K (1958) Biometrika 45:229
10. Adams BL, Zhao J, Grimmer H (1990) Acta Cyrst A 46(7):620
11. Brandon D (1966) Acta Metall 14:1479
12. Butler EP, Swann PR (1976) Acta Metall 24:343
13. Unwin PNT, Nicholson RB (1969) Acta Metall 17:1379